Spots on the surface of Betelgeuse

Results from new 3D stellar convection models

Freytag, Bernd; Steffen, Mathias; Dorch, Bertil

Published in:
Astronomical Notes - Astronomische Nachrichten

DOI:
10.1002/1521-3994(200208)323:3/4<213::AID-ASNA213>3.0.CO;2-H

Publication date:
2002

Document version:
Final published version

Astron. Nachr./AN **323** (2002) 3/4, 213–219

Spots on the surface of Betelgeuse — Results from new 3D stellar convection models

B. FREYTAG[1], M. STEFFEN[2], and B. DORCH[3]

[1] Department for Astronomy and Space Physics at Uppsala University, Box 515, SE 75120 Uppsala, Sweden
[2] Astrophysikalisches Institut Potsdam, An der Sternwarte 16, D-14482 Potsdam, Germany
[3] Astronomical Observatory (NBIfAFG), Juliane Maries Vej 30, 2100 Copenhagen Ø, Denmark

Received 2002 May 10; accepted 2002 July 3

Abstract. The observed irregular brightness fluctuations of the well-known red supergiant Betelgeuse (α Ori, M2 Iab) have been attributed by M. Schwarzschild (1975) to the changing granulation pattern formed by only a few giant convection cells covering the surface of this giant star. The surface structure revealed by modern interferometric methods appears to be generally consistent with the explanation as large-scale granular intensity fluctuations. The interferometric data can be modeled equally well by assuming the presence of a few (up to 3) unresolved hot or cool spots on a limb-darkened disk. In an effort to improve our theoretical understanding of the Betelgeuse phenomena, we have applied a new radiation hydrodynamics code (CO^{5}BOLD) to the problem of global convection in giant stars. For this purpose, the "local box" setup usually employed for the simulation of solar-type surface convection cannot be used. Rather, we have chosen a radically different approach: the whole star is enclosed in a cube ("star-in-a-box" setup). The properties of the stellar model are defined by the prescribed gravitational central potential and by a special inner boundary condition which replaces the unresolved core, including the source of nuclear energy production. We present current results obtained from this novel generation of 3D stellar convection simulations, proceeding from a toy model ("Mini-Sun") towards the numerically more demanding supergiant regime. We discuss the basic observational properties of Betelgeuse in the light of our best model obtained so far ($T_{\rm eff} = 3300$ K, $\log g = -0.4$). Finally, we describe a first attempt to investigate the interaction of the global convective flows with magnetic fields based on the kinematic approximation.

Key words: methods: numerical – stars: individual (Betelgeuse) – stars: spots – supergiants

1. Introduction

Betelgeuse (α Ori), a M2 Iab red supergiant, is among the stars with the largest apparent diameters. Its fundamental parameters are observationally not well determined: The parallax measured by Hipparcos is 7.6 ± 1.6 mas (131 pc with a considerable error). The measured angular diameter depends on wavelength, time, and assumptions about limb-darkening. With 4 m class telescopes (WHT and COAST, see references below) values between 42.6 mas and 76 mas at various wavelengths between 546 and 905 nm have been derived. Dyck et al. (1998) give a uniform disk diameter of 44.2 ± 0.2 mas at 2.2 μm. With a bolometric flux of $1.15\,10^{-11}$ W cm^{-2} μm^{-1} they derive an effective temperature of 3600 K. Radius and mass are not well known. Gray (2000) favors a radius of "some 800" solar radii and a mass between 10 and 20 solar masses. As an M2 giant, Betelgeuse lies close to the Hayashi limit in the Hertzsprung-Russell diagram, and hence is almost fully convective.

It has been possible to take direct images of Betelgeuse with HST (Gilliland & Dupree, 1996). These images, taken in the UV at 278 nm, show that the extended chromosphere deviates significantly from spherical symmetry. Spectrophotometric measurements reveal that Betelgeuse is an irregular variable. Its visual brightness changes by roughly a factor of two, and its radial velocity varies by ± 3 km/s (Goldberg, 1984). The variations are clearly not harmonic but rather more stochastic, and have been attributed by M. Schwarzschild (1975) to the changing brightness of only a few giant convection cells being present at the surface of this giant star, possibly superimposed on some kind of pulsation.

Betelgeuse has been monitored by interferometric methods for about one decade. These observations reveal an irregular shape of the image of Betelgeuse, the possible imprint of giant convection cells. The observational data can be fitted

Correspondence to: Msteffen@aip.de
For movies: Follow the links on the publishers web-pages.
http://www3.interscience.wiley.com/cgi-bin/jtoc?ID=60500255
as well as on the web-pages of the editorial office:
www.aip.de/AN/movies/

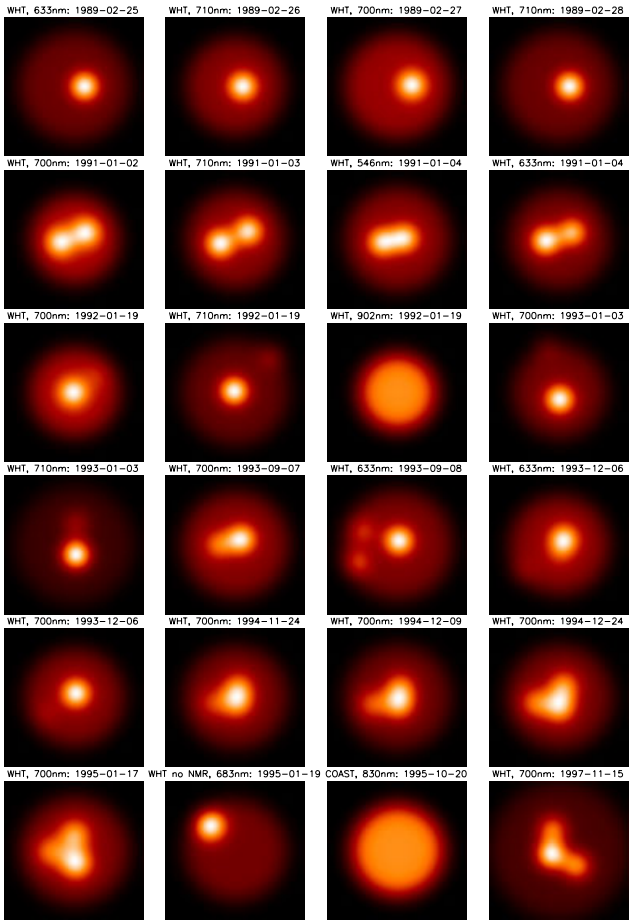

Fig. 1. WHT and COAST interferometric observations in the visible and near IR. The images were compiled from published data of spot positions and intensities, covering a time interval of almost 9 years (for references see text).

by a model consisting of a circular, limb-darkened disk with a small number of unresolved bright spots, as visualized in Fig. 1, based on published data of spot positions and intensities (Buscher et al., 1990; Wilson et al., 1992; Tuthill et al., 1997; Wilson et al., 1997; Klueckers et al., 1997; Burns et al., 1997; Young et al., 2000). The position and brightness of the spots changes only slightly during one month, but drastically on time scales of years.

Recently, Young et al. (2000) have demonstrated that the interferometric data may be fitted equally well with a model consisting of a disk with *dark* spots. The physical nature of the spots remains therefore unclear. For a better understanding of the phenomena seen at the surface of Betelgeuse, observations with higher spatial resolution and/or hydrodynamical simulations of global convection in a supergiant envelope would certainly be very helpful. In the following, we describe first results obtained from new 3D stellar convection models.

2. Numerical simulation of stellar convection

The numerical simulations described below have been performed with a new code named CO^{5}BOLD ("COnservative COde for the COmputation of COmpressible COnvection in a BOx of L Dimensions, L=2,3"), which is described more fully by Freytag (2002). It is based on a *finite volume approach* in a Cartesian box, and relies on operator (directional) splitting to reduce the multi-dimensional problem to 1D. In the 1D step, an approximate Riemann solver of Roe type is employed, modified to account for a realistic equation of state, a non-equidistant grid, and the presence of source terms due to an external gravity field. Reconstruction schemes of different order can be chosen. In addition, an optional 2D or 3D tensor viscosity can be activated for improved stability.

Non-local radiation transport is treated in a separate sub time step by solving the transfer equation on a system of rays with different directions, taking into account realistic tabulated opacities. So far, strict LTE is assumed (no scattering), and the effect of radiation pressure is ignored.

CO^{5}BOLD has two modes of operation. In the *local box* setup, a constant external gravity field is imposed in the $-z$ direction. The lateral boundaries are periodic, bottom and top boundaries are open and transmitting, respectively (for details see Freytag 2002). The solution of the radiative transfer is based on a Feautrier scheme applied to a system of *long* rays. This setup is used for the simulation of solar-type surface convection.

In the *star-in-a-box* setup, a fixed external central potential of the form

$$\Phi = -\frac{G\,M_*}{\left[r_0^4 + r^4/\sqrt{1+(r/r_1)^8}\right]^{1/4}} \qquad (1)$$

is applied, where M_* is the mass of the star to be modeled; r_0 and r_1 are free smoothing parameters. As long as $r_0^4 \ll r^4 \ll r_1^4$, $\Phi = -\frac{G\,M_*}{r}$. For $r \to 0$, $\Phi \to -\frac{G\,M_*}{r_0}$, and for $r \to \infty$, $\Phi \to -\frac{G\,M_*}{r_1}$. Typically, the inner smoothing radius is $r_0 \approx 0.2 R_*$. Inside a sphere of radius r_0, the internal energy is adjusted to keep the entropy close to some prescribed value. This replaces the energy production by nuclear fusion in the real stellar core. The parameter r_1 can be used to flatten the potential in the corners of the computational box to limit the drop in density. In this setup, all outer boundaries are transmitting for waves. The solution of the radiative transfer problem is based on a short-characteristics scheme. The *star-in-a-box* setup is used for the simulation of global convection in supergiants.

2.1. Local models: solar-type granulation

The solar convection zone is highly stratified: one of the consequences is that the convective turnover time scale changes by 4 orders of magnitude from the surface ($\tau_{\rm to}^{\rm top} \approx 200$ s) to the bottom of the convection zone ($\tau_{\rm to}^{\rm bot} \approx 25$ d). Moreover, the spatial scale of the solar granulation ($x_{\rm gran} \approx 2000$ km) is much smaller than the solar radius ($R_\odot \approx 700\,000$ km). In view of these numbers, it is impossible to model the whole solar convection zone in a single simulation which at the same time has to account for large-scale global flows and resolve the small-scale structures at the surface.

For this reason, hydrodynamical simulations of solar-type granular convection are typically restricted to local models, covering only a small section of the uppermost layers of the

deep convection zone. It is important to note that these models enclose the transition from the optically thick convective layers to the optically thin photosphere, where the plasma ascending from the solar interior looses its energy by efficient radiative cooling within a very narrow thermal boundary layer. The cool downdrafts generated at the surface by radiative cooling actually drive the flow. In fact, the properties of the entire convection zone are largely determined by the radiation hydrodynamics of the surface layers. For this reason, local simulations with realistic input physics turned out to be a very successful tool to study the solar granulation (e.g. Nordlund 1982; Steffen et al. 1989; Asplund et al. 2000; Skartlien et al. 2000; Stein & Nordlund 2000) and stellar surface convection (e.g. Ludwig et al. 1994, 1999; Freytag et al. 1996; Freytag & Salaris 1999), even though they are much smaller than the whole convection zone. A few examples of such *local box* models computed recently with the CO^{5}BOLD code are displayed in Fig. 2.

Among other things, the *local box* simulations of stellar surface convection have been used to investigate the size of stellar granules, $x_{\rm gran}$, as a function of stellar parameters. It turns out that, to a good approximation, $x_{\rm gran}$ scales with the pressure scale height at the surface. Roughly, $x_{\rm gran} \approx 10\mathcal{R}T_{\rm eff}/g$ (Freytag et al. 1997; $\mathcal{R}$ is the universal gas constant), which is equivalent to

$$\frac{x_{\rm gran}}{R_*} \approx 0.0025 * \frac{R_*}{R_\odot} \frac{T_{\rm eff,*}}{T_{\rm eff,\odot}} \frac{M_\odot}{M_*}. \qquad (2)$$

2.2. Global models: Supergiant convection

Substituting the stellar parameters of Betelgeuse into Eq (2), we obtain $x_{\rm gran}/R_* \approx 0.1$, implying the presence of a few hundred convection cells at the surface of this star. Under these conditions, the *star-in-a-box* approach becomes feasible.

3. State-of-the-art results

3.1. Toy supergiant: mini-Sun

In order to verify the *star-in-a-box* approach and to produce first test models, we have started with a scaled-down supergiant. The idea is to keep the solar surface parameters ($T_{\rm eff} = 5770$ K, $\log g = 4.44$) which are known to be numerically well tractable, but to reduce the stellar radius to $R_* \approx 2\,000$ km, such that $x_{\rm gran}/R_* \approx 1$ by design. The central potential of this toy model is characterized by $M_* = 8.2\,10^{-6}$ M$_\odot$ and $r_0 = 0.3R_*$, the specific entropy enforced in the central core is $1.73\,10^9$ erg/g/K. The initial model is a hydrostatic sphere with an adiabatic interior and an atmosphere in radiative equilibrium, perturbed by tiny random velocity fluctuations.

Fig. 3 shows the resulting time sequence from the very start. Initially, the luminosity of the model drops as the envelope cools because the convective energy supply from the deep interior is not yet established. After about 400 s, the convective instability has led to the formation of many small

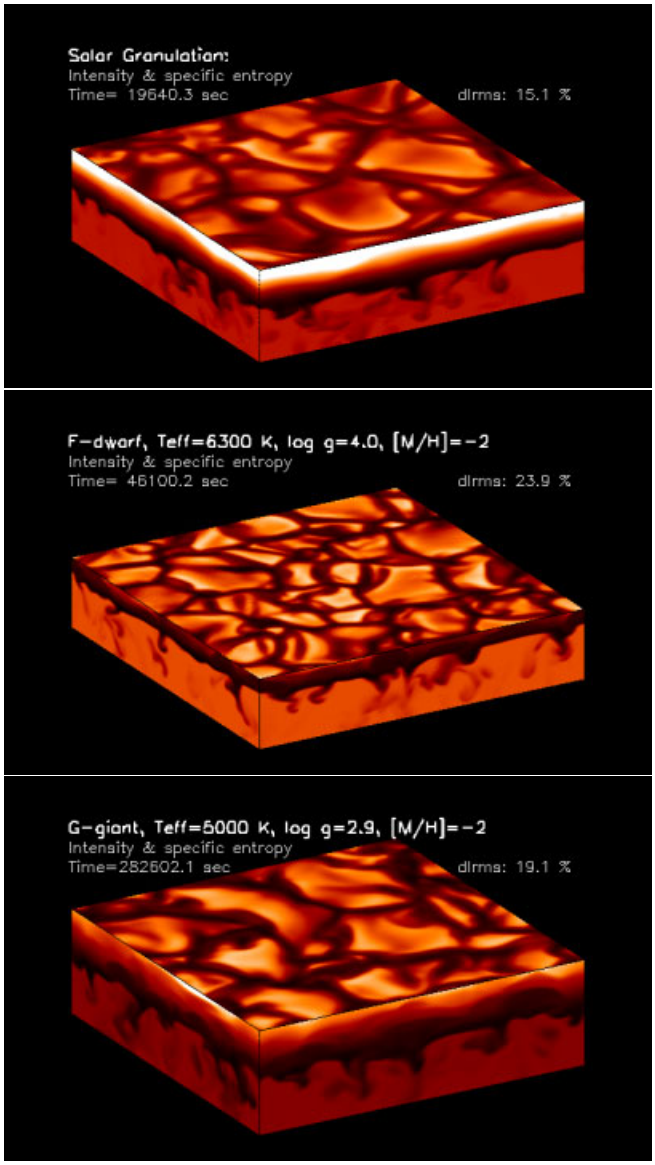

Fig. 2. Snapshots from 3D local box simulations of stellar surface convection performed with the CO^{5}BOLD code. **Top:** Solar Granulation ($T_{\rm eff} = 5770$ K, $\log g = 4.44$, [M/H]=0, dimension: 5.6 x 5.6 x 2.25 Mm, grid: 140 x 140 x 150), **Middle:** Metal-poor F-dwarf ($T_{\rm eff} = 6300$ K, $\log g = 4.0$, [M/H]=-2, dimension: 28.6 x 28.6 x 7.0 Mm, grid: 140 x 140 x 122), **Bottom:** Metal-poor G giant ($T_{\rm eff} = 5000$ K, $\log g = 2.9$, [M/H]=-2, dimension: 126 x 126 x 47 Mm, grid: 140 x 140 x 122). The panels show emergent intensity at $\lambda\,6200$ Å (top face) and specific entropy (side faces of simulation volume).

'granules' which become visible as bright spots at the surface. As time proceeds, the small cells quickly merge to form larger convection cells. Finally, the typical solar granulation pattern has formed, consisting of bright granules and a network of dark intergranular lanes, wrapped around a moon-sized object. By design, only a few convection cells occupy the surface.

In the later stages of this simulation, a new (unwanted) convective mode begins to dominate the convective flow, with a jet penetrating through the center from one hemisphere to the other, leading to a more irregular surface structure. As

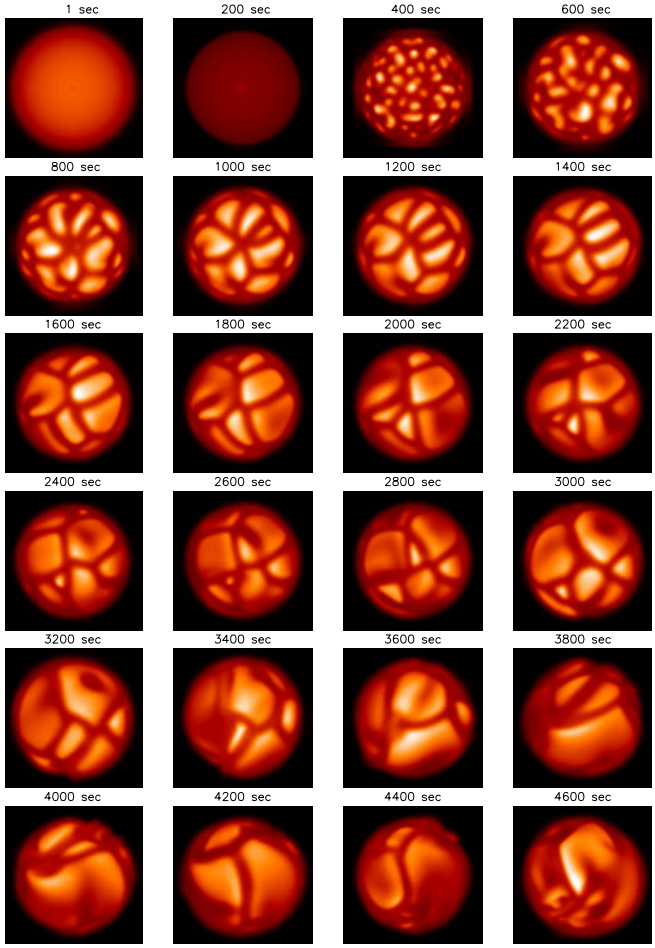

Fig. 3. Sequence of grey surface intensity ($\lambda \approx 6200$ Å) snapshots from the "mini-Sun" simulation. Surface parameters are $T_{\rm eff} = 5770$ K, $\log g = 4.44$; resolution: 127^3 cells.

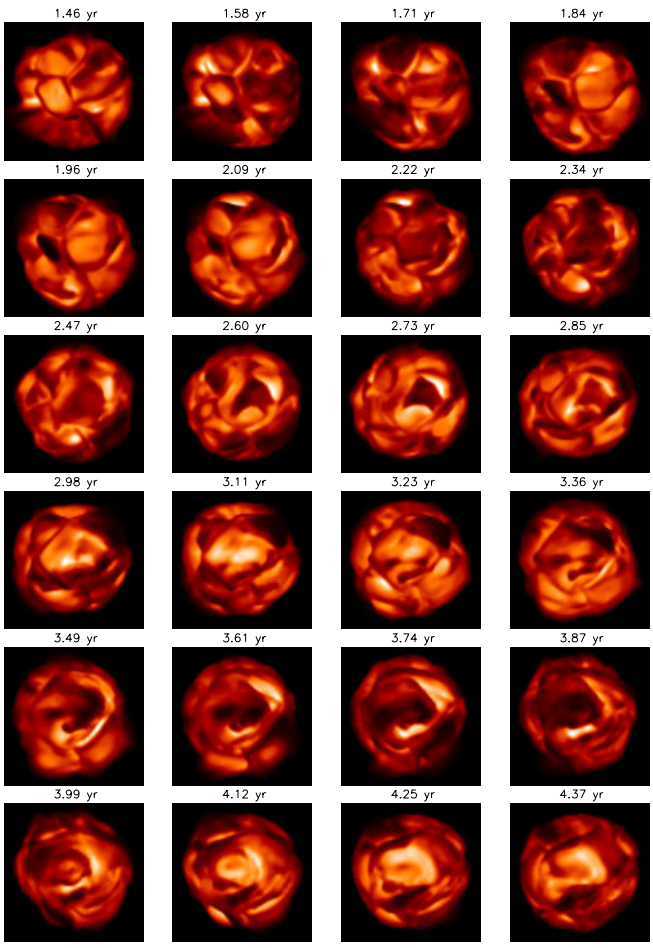

Fig. 4. Sequence of grey surface intensity ($\lambda \approx 6200$ Å) snapshots from the best red supergiant simulation obtained so far. Surface parameters are $T_{\rm eff} = 3340$ K, $\log g = -0.47$; resolution: 171^3 cells.

this mode continued to grow, we have stopped this sequence. While this model is not appropriate to provide new insights into the physics of supergiant convection, it serves to demonstrate the validity of the 'star-in-a-box' approach.

3.2. A (more) realistic red supergiant convection model

Starting from the "mini-Sun", we have successively changed the stellar parameters from solar towards lower $T_{\rm eff}$ and lower $\log g$. Such simulations become increasingly more difficult, numerically, because (i) the ratio of radiative to hydrodynamic time scale decreases (by roughly a factor of 100 from the Sun to a red supergiant), (ii) the convective velocities increase and hence the Mach number becomes larger, and (iii) the entropy jump at the surface becomes larger and steeper due to the dramatic rise of the opacity just below the photosphere.

The simulation that currently comes closest to Betelgeuse is characterized by the parameters $T_{\rm eff} \approx 3\,340$ K, $\log g \approx -0.47$, $R_*/R_\odot \approx 640$, $L_*/L_\odot \approx 46\,000$, $M_*/M_\odot = 5$, computed on a grid with 171^3 cells. A sequence of snapshots from this simulation is shown in Fig. 4. An animation of this sequence, covering a larger time interval, gives a better impression of the underlying dynamics (http://www.aip.de/ ~mst/pub_files/tmp/st35gm04n04_I2blm.mpg).

3.2.1. Surface structure, 'hot spots'

The surface structure seen in the intensity sequence (Fig. 4) appears clearly distinct from the solar granulation pattern. It is not simply composed of "bright granules and dark intergranular lanes". Due to interaction with the pulsation, entire giant convection cells can become significantly darker than the average surface intensity, and sometimes are surrounded by narrow bright lanes, giving the impression of a locally 'inverted' convection pattern. Occasionally, bright features ('hot spots') arise, preferentially at the edges of particularly dark cells. This is in line with observational evidence which indicates that the occurrence of hot spots tends to be correlated with a low overall brightness of the star (Gray 2000). At low spatial resolution, the simulated surface structure may well appear as a stellar disk with a few bright and/or cool spots. In this respect the simulations seem to be consistent with the interferometric observations mentioned in Sect. 1

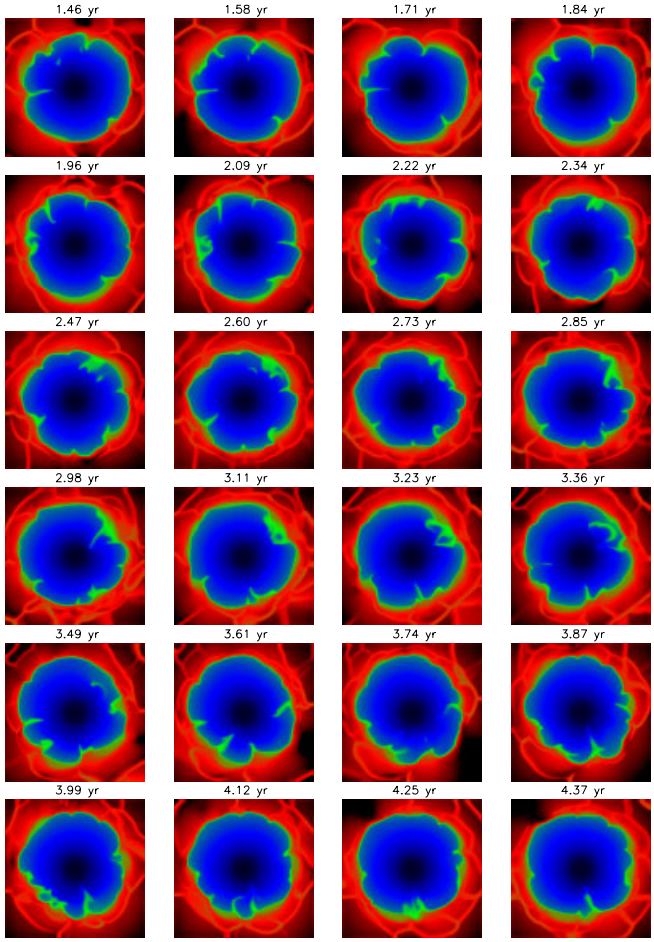

Fig. 5. Sequence of temperature slices through the center for the same sequence as shown in Fig. 4. Temperature ranges from 1 500 K to 150 000 K. Note the shock waves running into the outer atmosphere, moving mainly in the radial direction.

3.2.2. Atmospheric dynamics and giant convection cells

From a close inspection of animated intensity sequences (see above), we find that the convective flows are strongly modulated by global stellar oscillations. Clearly, deviations from a spherically symmetric configuration are significant. As a consequence of the variable surface brightness distribution, the photometric center of the unresolved stellar image moves in a stochastic way. While the shape of the star changes noticeably, surface area variations are of minor importance (see Fig. 6).

Atmospheric velocities are large, often exceeding 20 km/s, corresponding to Mach numbers of 5 up to 7. Therefore, turbulent pressure plays an important role for the average stratification of the stellar atmosphere. Shock waves running into the outer atmosphere are ubiquitous (see Fig. 5). Most of the shocks start from the surface of a single convection cell and move approximately radially outward. Near the downdrafts, almost stationary radial 'accretion shocks' are often seen.

It is difficult to estimate the size and number of convective elements from the surface intensity pattern (Fig. 4), because it is strongly affected by irregular non-radial pulsations and hence is not a good representation of the convective flow pattern. The temperature slices (Fig. 5), however, provide additional information. Typically they show 3 to 7 *deep-reaching downdrafts*, which corresponds to the number of giant convection cells occupying one hemisphere at a certain time. Simple scaling from the Sun based on the local pressure scale height predicts *several hundred* 'granules' at the surface of Betelgeuse (see Sect. 2.2, Eq.(2)), which may explain part of the small-scale structure seen in the simulations.

There are several physical reasons, however, that can explain the existence of the giant convection cells: first, the relatively short radiative time scales lead to an efficient damping of small scale temperature fluctuations and favor the formation of larger structures. In addition, the pressure scale height increases quickly with depth, and deep-reaching downdrafts 'sense' these layers instead of the very surface layers. As already noted by Schwarzschild (1975), the superadiabatic temperature gradient has high values over a much larger range of depth than in the Sun, again favoring large-scale flows.

On the other hand, the relatively poor numerical resolution in particular of the steep temperature drop at the surface may play a role: while models with an increased number of grid points and lowered numerical viscosity still show only a few giant convective elements dominating the outer envelope, smaller and shallower short-lived cells are seen to form just below the photosphere. The brightness of neighboring small cells is correlated, still giving rise to very large-scale fluctuations.

3.2.3. Variability

The temporal variation of the spatially averaged, frequency-integrated intensity is shown in the lower curves of Fig. 6 for 6 different points of view, corresponding to the 6 different faces of the computational cube. The brightness variations are clearly irregular, and it is difficult to determine a dominant time scale. The shortest characteristic time scales (≈ 0.3 yrs) are below the typical lifetime of a convection cell ($\gtrsim 1$ yr), and are probably due to intensity fluctuations of the granulation pattern and/or small-wavelength non-radial pulsations. The mean brightness obtained from the simulation does not fluctuate by more than ± 30 %, which seems to be consistent with the amplitude of the observed (visual) light curve.

Luminosity changes are somewhat smaller and contain less short-term fluctuations (second curve from top). Nevertheless, a dominant pulsation period is not easily inferred; possibly it is near $P \approx 1.5$ yrs. The upper curve demonstrates that surface area variations do not contribute significantly to the luminosity variations.

3.2.4. Magnetic dynamo action?

We have undertaken a first attempt to address the question whether the large-scale flow pattern emerging from our radiation hydrodynamical simulations of supergiant convection

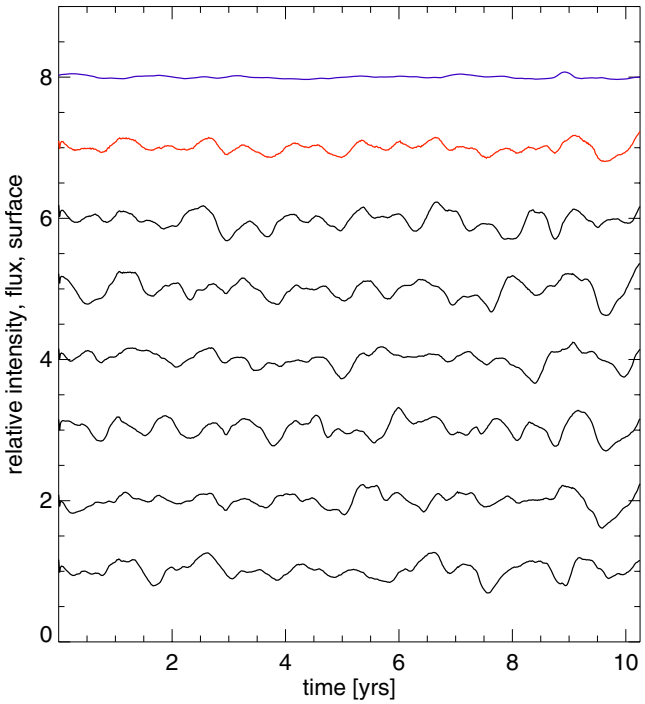

Fig. 6. Relative surface intensities (shifted by 0,1,2,3,4,5) as viewed from 6 different directions (lower 6 curves), normalized and shifted total flux (second from top), and an estimate of the relative surface area, $A \sim \langle R_* \rangle^2$ (upper curve), for the simulation displayed in Figs. 4 and 5.

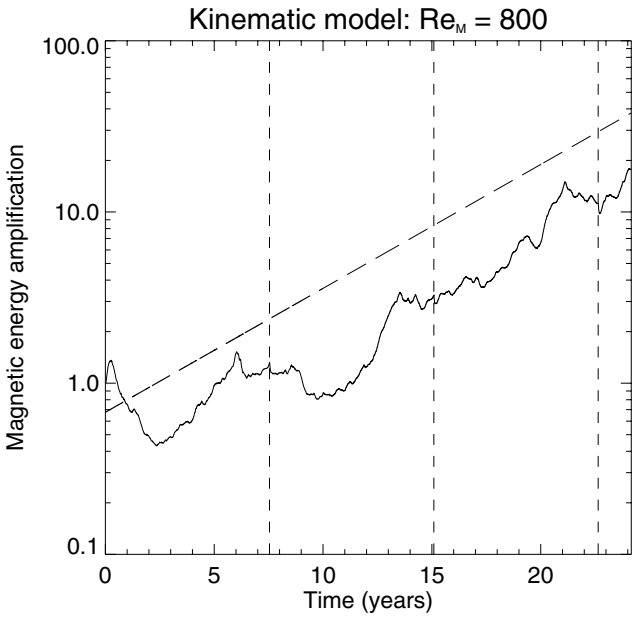

Fig. 7. Temporal evolution of the volume-integrated magnetic energy, $E_{\rm m}$, obtained from the solution of the induction equation, Eq.(3) for a prescribed velocity field $\boldsymbol{u}(x, y, z, t)$, taken from a radiation hydrodynamical simulation similar to that shown in the previous figures. A 'quenched' magnetic diffusivity was used, such that $R_{\rm m,min} = 800$

can sustain a magnetic field. The idea is to solve the induction equation

$$\frac{\partial \boldsymbol{B}}{\partial t} = \nabla \times (\boldsymbol{u} \times \boldsymbol{B}) + \nabla \times (\eta \nabla \times \boldsymbol{B}) \qquad (3)$$

with a prescribed, time-dependent velocity field $\boldsymbol{u}(x, y, z, t)$ (kinematic approximation) as obtained from the convection simulations described in the previous sections. We note that the physical conditions in the interior of red supergiants imply low magnetic diffusivities in the range $\eta \approx 10^8 \ldots 10^6$ cm^2/s, compared to values of $\eta \approx 10^8$ cm^2/s in the solar surface layers. Due to the large scales of the velocity field, the corresponding magnetic Reynolds numbers are very high, $R_{\rm m} \approx 10^{10} \ldots 10^{12}$. The induction equation was solved using the code by Galsgaard, Nordlund and others (see e.g. Galsgaard & Nordlund 1997), which has previously been employed in the context of kinematic dynamo action (e.g. Dorch 2000). The numerical method used was a 6th order staggered mesh scheme involving quenched magnetic diffusion coefficients allowing large values of $R_{\rm m}$ in the bulk of the flow, localizing Reynolds number minima of $R_{\rm m,min}$ to regions of the flow where the convergence across field lines are large. The solution of the induction equation was therefore carried out with the highest numerically acceptable $R_{\rm m} \gg R_{\rm m,min} = 800$ in the bulk of the flow; only in regions with strong gradients of the magnetic field, $R_{\rm m}$ is actually reduced to a minimum value of 800.

We solve Eq.(3) starting with a weak seed magnetic field; it turns out that the results are independent of whether the initial magnetic field is chosen to be unidirectional or small-scale periodic. We compute the temporal evolution of the volume-integrated magnetic energy, $E_{\rm m} = \int_V \boldsymbol{B}^2/(8\pi)\,{\rm d}V$. The result is shown in Fig. 7: we observe an exponential growth of the total magnetic energy over the whole available time interval of about 25 yrs, which corresponds to roughly 20 convective turnover time scales. This result is largely independent of the assumed geometry (unidirectional or random orientation) and spatial scale of the initial field. However, we find positive growth rates only as long as $R_{\rm m,min} \gtrsim 500$. Even though the covered time interval is much shorter than one diffusion time scale (corresponding to the largest scales), the fact that $E_{\rm m}$ grows *exponentially* suggests that the giant-cell convection probably constitutes a fast dynamo flow, implying that Betelgeuse is likely to have a magnetic field.

Note that this kind of dynamo works even without stellar rotation. It is of the same nature as the local dynamo possibly contributing to the small-scale magnetic field at the solar surface (cf. Cattaneo 1999), but is fundamentally different from the global dynamo thought to be responsible for the activity cycles in solar-type stars.

Further investigations are clearly necessary to corroborate this conclusion, to estimate the resulting strength of the magnetic field, and to find out whether the magnetic field might form star spots or otherwise influence the observable surface structure.

4. Conclusions

The main purpose of this paper is to demonstrate that 3-dimensional 'star-in-a-box' simulations of global supergiant convection are now becoming feasible. The preliminary models presented here include a realistic equation of state, and

non-local radiative transfer with realistic opacities. The stellar parameters of the most advanced models already come close to the regime of real red supergiants.

Our simulations show that convection in a red supergiant ($T_{\rm eff} \approx 3\,300$ K, $\log g \approx -0.4$) is indeed dominated by only a few giant convection cells, as suggested by Schwarzschild (1975). Changes of the convective flow together with superimposed non-radial pulsations give rise to irregular brightness variations, significant deviations from spherical symmetry, and variations of the surface structure (bright spots). Atmospheric velocities are found to be large, Mach numbers of 5 are easily reached, leading to the formation of shock which propagate into the outer atmosphere and may play a role in heating the chromosphere. The appearance of the supergiant granulation seems to be more complex than the well-known solar granulation pattern, probably due to a substantial modulation by stellar pulsations, and also due to a different temperature dependence of the radiative opacity.

The current radiation hydrodynamical convection models seem to be in basic agreement with available photometric and interferometric observations. They even can account for the observation that bright spots tend to be associated with periods of low overall stellar brightness.

5. Future plans

Further improvements of the code in terms of speed, stability, resolution, and microphysics are necessary to allow more realistic simulations of global convection in red supergiants. From the physics point of view, it would be desirable to account for the frequency-dependence of radiative transfer and to include scattering and the dynamical effect of radiation pressure. It might also be important to compute the gravitational potential in a self-consistent way. If dust formation can be included, improved simulations may also serve to study the mass loss phenomenon. The effect of stellar rotation can easily be included as long as it is slow.

It will be of great interest to compute synthetic line profiles from the global convection models for comparison with spectroscopic observations. In this way it will be possible to check whether the observed variations of the line profile (radial velocity, strength, shape) can be explained by the current non-magnetic convection models.

Acknowledgements. Computations were carried out at the computer center of the university in Kiel, at TAC in Copenhagen, and on the Sun cluster at Ångström laboratory in Uppsala.

References

Asplund, M., Ludwig, H.-G., Nordlund, Å., Stein, R.F.: 2000, A&A 359, 66
Burns, et al.: 1997, MNRAS 290, L11
Buscher, D.F., Haniff, C.A., Baldwin, J.E., Warner, J.P.: 1990, MNRAS 245, 7p
Cattaneo, F.: 1999, ApJ 515, L39
Dorch, S.B.F.: 2000, PhyS 61, 717
Dyck, H.M., van Belle, G.T., Thompson, R.R.: 1998, ApJ 116, 981
Freytag, B., Steffen, M., Ludwig, H.-G.: 1996, A&A 313, 497
Freytag, B., Holweger, H., Steffen, M., Ludwig, H.-G.: 1997, in: F. Paresce (ed.), *Science with the VLT Interferometer*, ESO Astrophysics Symposia, Springer, p. 316
Freytag, B., Salaris, M.: 1999, ApJ 513, L49
Freytag, B.: 2002, A&A, in preparation
Galsgaard, K., Nordlund, Å.: 1997, JGR 102, 219
Gilliland, R.L., Dupree, A.K.: 1996, ApJ 463, L29
Goldberg, L.: 1984, PASP 96, 366
Gray, D.F.: 2000, ApJ 532, 487
Klueckers, et al.: 1997, MNRAS 284, 711
Ludwig, H.-G., Jordan, S., Steffen, M.: 1994, A&A 284, 105
Ludwig, H.-G., Freytag, B., Steffen, M.: 1999, A&A 346, 111
Nordlund, Å.: 1982, A&A 107, 1
Schwarzschild, M.: 1975, ApJ 195, 137
Skartlien, R., Stein, R.F., Nordlund, Å.: 2000, ApJ 541, 468
Steffen, M., Ludwig, H.-G., Krüß, A.: 1989, A&A 213, 371
Stein, R.F., Nordlund, Å.: 2000, SoPh 192, 91
Tuthill, et al.: 1997, MNRAS 285, 529
Wilson, et al.: 1992, MNRAS 257, 369
Wilson, et al.: 1997, MNRAS 291, 819
Young, J.S., Baldwin, J.E., Boysen, R.C., et al.: 2000, MNRAS 315, 655